

# The Teddy-Tool v1.1: temporal disaggregation of daily climate model data for climate impact analysis

Florian Zabel<sup>1</sup>, Benjamin Poschlod<sup>2</sup>

<sup>1</sup>Ludwig-Maximilians-Universität München (LMU), Department of Geography, Luisenstr. 37, 80333 Munich, Germany

<sup>2</sup>Research Unit Sustainability and Climate Risks, Center for Earth System Research and Sustainability, Universität Hamburg, Grindelberg 5, 20144 Hamburg, Germany

Correspondence to: Florian Zabel (f.zabel@lmu.de)

## Abstract

Climate models provide required input data for global or regional climate impact analysis in [temporally aggregated form](#), often [in daily resolution](#) to save space on data servers. Today, many impact models work with daily data, however, sub-daily climate information is getting increasingly important for more and more models from different sectors, such as the agricultural, the water, and the energy sector. Therefore, the open source Teddy-Tool ([temporal disaggregation of daily climate model data](#)) has been developed to disaggregate (temporally downscale) daily climate data to sub-daily hourly values. [Here](#), we describe and [validate](#) the temporal disaggregation, which is based on [the choice of daily climate analogues](#). [In this study, we apply the Teddy-Tool to disaggregate bias-corrected climate model data from the Coupled Model Intercomparison Project Phase 6 \(CMIP6\). We choose to disaggregate temperature, precipitation, humidity, longwave radiation, shortwave radiation, surface pressure, and wind speed. As a reference, globally available bias-corrected hourly reanalysis WFDE5 data from 1980-2019 are used to take specific local and seasonal features of the empirical diurnal profiles into account. For a given location and day within the climate model data, the Teddy-Tool screens the reference data set to find the most similar meteorological day based on rank statistics. The diurnal profile of the reference data is then applied on the climate model.](#) The physical dependency between variables is preserved, since the diurnal profile of all variables is taken from the same, most similar meteorological day of the historical reanalysis dataset. [Mass and energy are strictly preserved by the Teddy-Tool to exactly reproduce the daily values from the climate models.](#)

[For evaluation, we aggregate the hourly WFDE5 data to daily values and apply the Teddy-Tool for disaggregation. Thereby, we compare the original hourly data with the data disaggregated by Teddy.](#) We perform a sensitivity analysis of different time window sizes used for finding the most similar meteorological day in the past. In addition, we perform a cross-validation [and](#) autocorrelation analysis for 30 globally distributed samples around the world, representing different climate zones. The validation shows that Teddy is able to reproduce historical diurnal courses with high correlations >0.9 for all variables, except for wind speed (>0.75) and precipitation (>0.5). [We discuss limitations of the method regarding the reproduction of precipitation extremes, inter-day connectivity, and disaggregation of end-of-century projections with strong warming. Depending on the use case](#), sub-daily data provided by the Teddy-Tool could make climate impact assessments more robust and reliable.

## 1. Introduction

Gelöscht: 0

Gelöscht: on a daily basis

[5] nach unten verschoben: Thereby, mass and energy are strictly preserved by the Teddy-Tool to exactly reproduce the daily values from the climate models.

Gelöscht: for temperature, precipitation, humidity, longwave radiation, shortwave radiation, surface pressure and wind speed.

Gelöscht: document

Formatiert: Schriftfarbe: Automatisch

Gelöscht:

Gelöscht: Therefore

Formatiert: Schriftfarbe: Automatisch

Gelöscht: course

Gelöscht: empirically

Gelöscht: Thereby,

[5] verschoben (Einfügung)

Gelöscht: mMass and energy are strictly preserved by the Teddy-Tool to exactly reproduce the daily values from the climate models.

Gelöscht:

Gelöscht: ,

Gelöscht: and extreme value

Gelöscht: However,

Gelöscht: w

Gelöscht: also

Gelöscht: Consequently

Formatiert: Schriftart: Fett

Formatiert: Listenabsatz, Nummerierte Liste + Ebene: 1 + Nummerierungsformatvorlage: 1, 2, 3, ... + Beginnen bei: 1 + Ausrichtung: Links + Ausgerichtet an: 0,63 cm + Einzug bei: 1,27 cm

65 Sub-daily climate data is becoming increasingly important in climate impact analysis. This type of data,  
66 which captures variations in temperature, precipitation, and other weather variables at intervals of  
67 less than a day, can provide a more detailed representation of local and regional climate conditions  
68 and temporal variations. This information can be crucial for evaluating the impacts of climate change  
69 on various sectors, such as agriculture, water resources, energy production, and human health (Golub  
70 et al., 2022; Trinanés and Martínez-Urtaza, 2021; Colón-González et al., 2021; Tittensor et al., 2021;  
71 Byers et al., 2018; Jägermeyr et al., 2021; Poschlod and Ludwig, 2021; Degife et al., 2021). A better  
72 representation of the diurnal course of temperature, extreme precipitation events, and other weather  
73 variables are also important for adaptation assessments which depend on behavior or processes with  
74 high temporal dynamics, such as the energy demand, labor activity, the heat stress of crops or flood  
75 events (Minoli et al., 2022; Zabel et al., 2021; Reed et al., 2022; Orlov et al., 2021; Franke et al., 2022;  
76 [Poschlod 2022](#)). Research has shown that using sub-daily climate data can result in more robust and  
77 reliable impact assessments compared to using daily data (Orlov et al. 2023).

78 Today, most climate model data are available for download at daily resolution because of the high  
79 storage requirements for sub-daily climate data ([Juckes et al., 2020](#)). However, the demand for sub-  
80 daily data is increasing [with future developments of data management expected to handle this](#)  
81 [demand with decreasing](#) costs for storage and computing resources ([Lüttgau & Kunkel, 2018](#)). Different  
82 methods exist to disaggregate available daily climate data to sub-daily, most often hourly values. These  
83 can be roughly divided into statistical methods, weather generators, and mechanistic approaches,  
84 although mixed forms also exist (Förster et al., 2016).

85 Mechanistic methods use regional climate models to dynamically downscale atmospheric conditions  
86 in time and space, usually for a limited area (Vormoor and Skaugen, 2013; Liu et al., 2011; Kunstmann  
87 and Stadler, 2005). Weather generators generate synthetic sequences of hourly weather variables by  
88 using random number generators that match statistics (Ailliot et al., 2015; Mezghani and Hingray,  
89 2009). Various statistical methods exist for temporal disaggregation of daily climate data, ranging from  
90 simple interpolations or deterministic approaches to non-parametric approaches and methods that  
91 derive statistical relationships from historical data [or look for climate analogues](#) ([Bennett et al., 2020](#);  
92 [Breinl and Di Baldassarre, 2019](#); [Chen, 2016](#); Debele et al., 2007; Förster et al., 2016; Görner et al.,  
93 2021; Liston and Elder, 2006; Park and Chung, 2020; Verfaillie et al., 2017; Poschlod et al., 2018; Zhao  
94 et al., 2021). Each of these methods has its own advantages and limitations, and the choice of method  
95 depends on factors such as the specific needs of the impact assessment, the quality of the available  
96 data, and computational resources.

97 Here, we introduce the Teddy-Tool (temporal disaggregation of daily climate model data), which uses  
98 statistical methods for temporal disaggregation of daily climate model data. Existing statistical  
99 approaches are often only valid for a specific location and cannot be applied globally. In addition,  
100 available disaggregation tools often focus on only one variable ([e.g. Pui et al., 2012](#)) and therefore do  
101 not consider physical interdependencies between different variables, such as precipitation, humidity,  
102 temperature, and radiation. Teddy has been specifically developed as a globally applicable tool for  
103 climate impact studies. For this purpose, Teddy strictly preserves mass and energy of daily climate  
104 model data for each variable throughout the disaggregation procedure. Teddy additionally aims at  
105 taking regional and seasonal climate characteristics into account and considers the physical  
106 consistency between variables.

Gelöscht: due to

Gelöscht: lower

109 Teddy represents an easy-to-use tool that can be applied for climate impact assessments in different  
 110 sectors that allows a physically consistent temporal disaggregation of daily climate model data. The  
 111 Teddy-Tool has been written in Matlab and is available open source via Zenodo ([see code availability](#)).

## 112 2. Data and data requirements

113 In principal, the Teddy-Tool can be used with any climate input, but has specifically been developed to  
 114 be used with daily climate data for historical time periods and future scenarios from the Inter-Sectoral  
 115 Impact Model Intercomparison Project (ISIMIP), which ISIMIP offers a framework for consistently  
 116 projecting the impacts of climate change across affected sectors and spatial scales (Warszawski et al.,  
 117 2014). To guarantee cross-sectoral consistency in ISIMIP, all sectors are provided with the same climate  
 118 data. ISIMIP provides bias-corrected climate model data from the Coupled Model Intercomparison  
 119 Project Phase 6 (CMIP6) and trend-preserving reanalysis climate data (Lange, 2019). Within ISIMIP,  
 120 some modeling communities from different sectors have expressed their need for sub-daily climate  
 121 data, including the agricultural and the energy sector.

122 Daily bias-corrected climate model data are provided by ISIMIP at 0.5° spatial resolution for air  
 123 temperature (tas), humidity (hurs), shortwave radiation (rsds), longwave radiation (rls), air pressure  
 124 (ps), wind speed (sfcwind), and precipitation (pr) (Lange, 2019). For air temperature, the daily  
 125 maximum (tasmax) and minimum (tasmin) values are additionally provided. ISIMIP provides CMIP6  
 126 data for the climate models GFDL-ESM4, IPSL-CM6A-LR, MPI-ESM1-2-HR, MRI-ESM2-0, and UKESM1-  
 127 0-LL.

128 Teddy requires hourly climate data as a reference for temporal disaggregation. Therefore, we use the  
 129 WFDE5 dataset, which has been generated using the WATCH Forcing Data (WFD) methodology applied  
 130 to ERA5 reanalysis data (Cucchi et al., 2020). The bias-adjusted hourly WFDE5 data is globally available  
 131 for the time period between 1979 and 2019 at 0.5° spatial resolution. It is consistent with the bias-  
 132 adjustment procedure within ISIMIP (Lange, 2019) and thus provides a consistent hourly reference  
 133 data for Teddy.

134 Table 1 gives an overview of the available variables and the required datasets at their temporal  
 135 resolution. The temporal resolution of the Teddy output is adjustable by the user and can be set to 1-  
 136 , 2-, 3-, 4-, 6-, 8-, or 12-hourly values.

137 Table 1: Variables and units of used hourly (h) and daily (d) climate data and the Teddy output. For  
 138 WFDE5, the specific variable name is provided in brackets. WFDE5 variables have instantaneous values,  
 139 while SWdown, LWdown, Rainf and Snowf have average values over the next hour at each time step.

Variable	WFDE5 (h)	ISIMIP Climate Model (d)	Teddy (flexible)
<u>tas</u>	<u>K (Tair)</u>	<u>K</u>	<u>K</u>
<u>tasmin</u>	<u>=</u>	<u>K</u>	<u>=</u>
<u>tasmax</u>	<u>=</u>	<u>K</u>	<u>=</u>
<u>hurs/huss</u>	<u>kg/kg (Qair)</u>	<u>%</u>	<u>%</u>
<u>rsds</u>	<u>W m<sup>-2</sup> (SWdown)</u>	<u>W m<sup>-2</sup></u>	<u>W m<sup>-2</sup></u>

[3] nach unten verschoben: In principal, the Teddy-Tool can be used with any climate input, but has particularly been used so far with bias corrected daily CMIP6 climate data

Gelöscht: the

Gelöscht: ISIMIP

Gelöscht: <https://doi.org/10.5281/zenodo.7679149>

Formatiert

Formatiert

[3] verschoben (Einfügung)

Gelöscht: particularly

Gelöscht: used

Gelöscht: so far

Gelöscht: bias corrected

Gelöscht: CMIP6

Gelöscht: (Eyring et al., 2016)

Gelöscht: ISIMIP (

Gelöscht: ,

Gelöscht: ,

Gelöscht: provides bias corrected and trend-preserved

Gelöscht: ed

Gelöscht: To guarantee cross-sectoral consistency, all

Gelöscht:

[2] verschoben (Einfügung)

Gelöscht: Teddy uses an empirical approach, which applie

Gelöscht: daily

Gelöscht: from

Gelöscht: the

Gelöscht: project

Gelöscht: for

Gelöscht: (tasmax, tasmin)

Gelöscht: different historical and future time periods and

Gelöscht: for the

Gelöscht:

Gelöscht: As a reference,

Gelöscht: globally available hourly bias-corrected reanaly

[4] verschoben (Einfügung)

Formatiert

Formatierte Tabelle

Formatiert

Formatiert

Formatiert

Formatiert

Formatiert

<u>rlds</u>	<u>W m<sup>-2</sup> (LWdown)</u>	<u>W m<sup>-2</sup></u>	<u>W m<sup>-2</sup></u>
<u>pr</u>	<u>kg m<sup>-2</sup> s<sup>-1</sup> (Rainf+Snowf)</u>	<u>kg m<sup>-2</sup> s<sup>-1</sup></u>	<u>mm timestep<sup>-1</sup></u>
<u>ps</u>	<u>Pa (PSurf)</u>	<u>Pa</u>	<u>hPa</u>
<u>sfcwind</u>	<u>m s<sup>-1</sup> (Wind)</u>	<u>m s<sup>-1</sup></u>	<u>m s<sup>-1</sup></u>

### 3. Methods

Teddy uses an empirical approach, which 1) selects the 'most similar meteorological day' for the daily climate model data (here: ISIMIP CMIP6 data) within the reference climate data (here: WFDE5) at the same location. 2) Teddy applies the location-specific diurnal course to each variable of the daily climate model data for a day of interest. In the following, the procedure is explained in detail, where the example case of ISIMIP climate data and WFDE5 reference data is used for further illustration:

In a first precalculation step, in order to minimize computational resources, hourly WFDE5 data are aggregated to daily values and stored as NetCDF files. The daily aggregation uses mean values for all variables and daily sums for precipitation. In addition, rainfall and snowfall fluxes must be summed up for WFDE5. Daily maximum and minimum temperature are calculated from the hourly data. Units of climate inputs are converted to match the Teddy output (see Tab. 1). For the conversion of specific humidity to relative humidity, the Buck equation is applied (Buck, 1981).

After reading the daily climate model data for the selected location (latitude/longitude) that determines a specific grid cell at 0.5° resolution, the daily mean values of all ISIMIP variables (see Tab. 1) are compared to the aggregated daily values of WFDE5 for a specific time step in order to identify the most similar meteorological day. For the comparison, a day-of-year (DOY) window can be selected by the user that allows for a selection of days around the DOY of the actual time step. By default, the DOY window size is set to 11, which means a sequence of ± 11 days around the actual DOY. As a result, 23 days are selected from each of the 40 WFDE5 reference years (1980-2019). These 920 days now serve as the statistical population for further calculations (Fig. 1). In a next step, the climate model day of interest and the statistical population of 920 WFDE5 days are classified according to their precipitation state (wet / dry). As climate models tend to produce too many days with low-intensity precipitation called 'drizzle bias' (Chen et al., 2021), days with aggregated daily precipitation values below 1 mm per day are considered as dry days (Sun et al., 2006). Depending on the precipitation state of the previous day, the day of interest and the following day, there are eight classes: dry-dry-dry, dry-dry-wet, wet-dry-dry, wet-dry-wet, dry-wet-dry, dry-wet-wet, wet-wet-dry, and wet-wet-wet. This step is included to better reproduce the inter-day connectivity of precipitation (Li et al., 2018). Only days with the same precipitation class as the climate model day of interest are selected for the further course. Next, the absolute error (AE) between daily climate model and aggregated daily WFDE5 data for each variable is calculated for the remaining statistical population and ranked in ascending order.

The ranking approach is chosen, since the absolute or relative errors of different meteorological variables cannot be compared to each other. The ranks are cumulated with equal weight over all variables for each day of the statistical population. In this context, we define 'the most similar meteorological day' as the day with the minimum sum of ranks (Fig. 1). Thus, the 'most similar meteorological day' refers to the statistical similarity of all available daily near-surface meteorological variables at a given location and time. The approach works under the assumption that similar daily

- Formatiert: Links
- Formatiert: Links
- Formatiert: Links
- Formatiert: Links
- Gelöscht: <#>¶
- Formatiert: Listenabsatz, Links, Nummerierte Liste + Ebene: 1 + Nummerierungsformatvorlage: 1, 2, 3, ... + Beginnen bei: 1 + Ausrichtung: Links + Ausgerichtet an: 0,63 cm + Einzug bei: 1,27 cm
- Formatiert: Schriftart: Fett
- Gelöscht: Temporal disaggregation¶
- Gelöscht: region
- Gelöscht: from the most similar meteorological day in the past
- [2] nach oben verschoben: Teddy uses an empirical approach, which applies the region-specific diurnal course from the most similar day in the past to daily climate model data for a day of interest. Teddy has been developed specifically to disaggregate daily bias-corrected climate model data from the ISIMIP project at 0.5° spatial resolution for air temperature (tas), humidity (hurs), shortwave radiation (rsds), longwave radiation (rlds), air pressure (ps), windspeed (sfcwind), and precipitation (pr) (Lange, 2019). For air temperature, the daily maximum and minimum values (tasmax, tasmin) are additionally provided. ISIMIP provides data for different historical and future time periods and scenarios for the climate models GFDL-ESM4, IPSL-CM6A-LR, MPI-ESM1-2-HR, MRI-ESM2-0, and UKESM1-0-LL.
- Gelöscht: The diurnal profile of the most similar ...
- Gelöscht: ¶
- [4] nach oben verschoben: Table 1: Variables and units
- Gelöscht: Variable ...
- Gelöscht: basic population
- Gelöscht: basic population
- Gelöscht: "
- Gelöscht: "
- Gelöscht: basic population
- Gelöscht: over all variables
- Gelöscht:
- Gelöscht: basic population
- Gelöscht: T
- Gelöscht: is determined
- Gelöscht: the lowest lowest cumulated ranks
- Formatiert: Englisch (Vereinigte Staaten)
- Gelöscht: '
- Formatiert: Englisch (Vereinigte Staaten)
- Formatiert: Englisch (Vereinigte Staaten)
- Gelöscht: Hence, it does not account for the large-scale ...

302 [values would have a similar sub-daily profile \(Li et al., 2018; Pui et al., 2012; Sharma et al., 2006\).](#)  
303 Finally, the hourly values are taken from the most similar **meteorological** day of the WFDE5 reference  
304 dataset for each variable and **are** divided by the WFDE5 daily mean **(sum for precipitation)** value of the  
305 selected day, in order to refer to relative diurnal profiles without absolute variations (Fig. 1). The hourly  
306 profile is then applied for each variable to the daily mean **(sum for precipitation)** value from the climate  
307 model. Thus, the daily mean **value (sum for precipitation) of the climate model is conserved and**  
308 **reproduced by the disaggregated values.**

309 For temperature, the resulting hourly temperature is further scaled between the provided minimum  
310 and maximum. The scaling is performed in a way that the daily mean value is preserved with an  
311 accuracy of four decimals. Relative humidity is limited to 100%, **considering the preservation of the**  
312 **daily mean value.**

313 Large selected DOY windows increase the **statistical population**, but on the other sight might distort  
314 climatic characteristics with a strong seasonal course such as shortwave radiation values for the actual  
315 DOY. Therefore, we preprocessed hourly potential (cloud free) solar radiation for each DOY globally at  
316 0.5° spatial resolution. This data is used as upper bound to limit the resulting hourly values for the  
317 corresponding DOY, while the daily mean value is preserved.

318 In a final step, **the** hourly values **are aggregated to the temporal resolution as set by the user.**

Gelöscht:

Gelöscht:

Gelöscht: is conserved

Gelöscht:

Gelöscht: again under

Gelöscht: preserving

Gelöscht: .

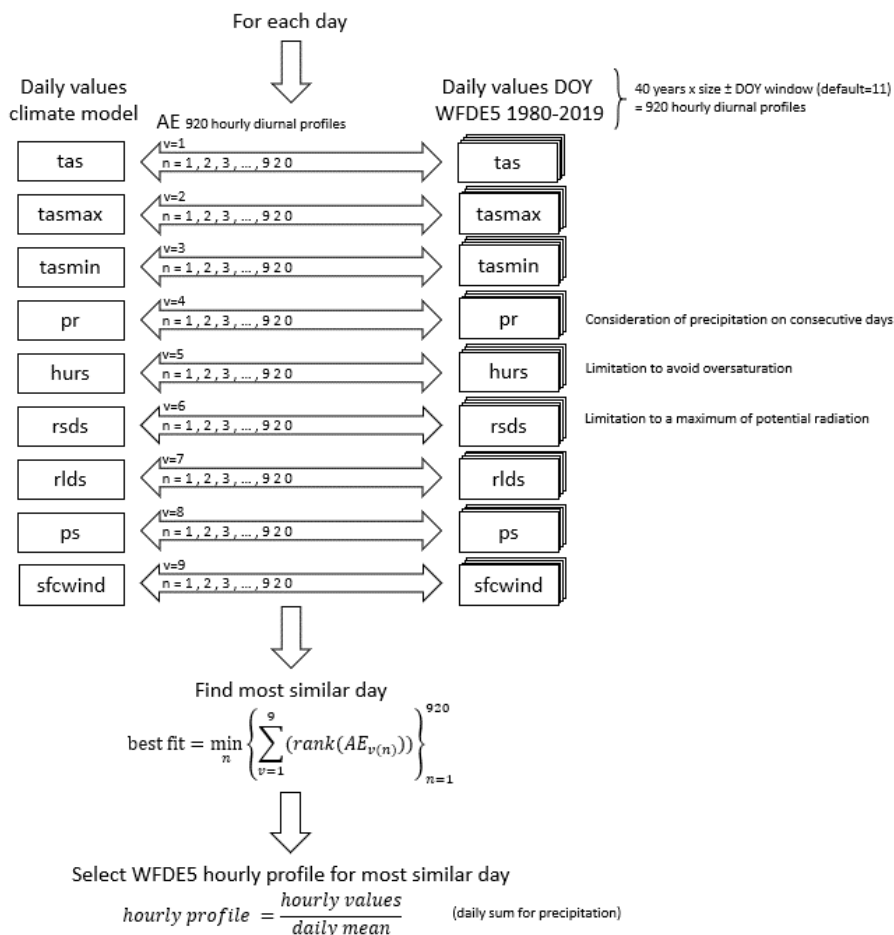
Gelöscht: basic population

Gelöscht:

Gelöscht: can again be aggregated to the time step set by the user

Gelöscht: (possible: 1, 2, 3, 4, 6, 8, 12)

Gelöscht:



332  
333 Figure 1: Procedure to identify the most similar meteorological day in the population of [WFDE5](#)  
334 reference data for the default DOY window of  $\pm 11$  days around the actual DOY.

335 In rare cases, precipitation cannot be distributed, due to [no](#) precipitation in the reference data. [This](#)  
336 [can happen in dry deserts, where 40 years of WFDE5 data show no precipitation record within the](#)  
337 [range of the moving DOY window \(Supplementary Fig. S1 shows a map where this is the case\).](#) To  
338 handle this exception, several options are implemented. First, the DOY window is automatically  
339 expanded to  $\pm 50$  days around the actual DOY [in order to increase the statistical population and thus](#)  
340 [the probability to include a precipitation event.](#) If [still no precipitation event is found in the reference,](#)  
341 a linear regression between the precipitation amount and the [precipitation](#) duration is performed for  
342 the specific location across the entire [available](#) data spectrum. The linear regression determines the  
343 usual duration of the selected precipitation event. Subsequently, an hour is randomly selected for the  
344 start of the precipitation event. [A goal of Teddy was to consider the physical consistency of inter-](#)  
345 [variable relationships. Precipitation generally affects other climate variables \(e.g. humidity, radiation,](#)  
346 [temperature, etc.; Meredith et al., 2021\).](#) During night, physical interdependencies between

- Gelöscht:** failing
- Gelöscht:** ure
- Formatiert:** Nicht Hervorheben
- Gelöscht:** see
- Formatiert:** Nicht Hervorheben
- Gelöscht:** ?
- Formatiert:** Nicht Hervorheben
- Gelöscht:**
- Gelöscht:** this doesn't help
- Formatiert:** Schriftfarbe: Automatisch

353 precipitation and other variables are generally lower, because radiation is not affected and less energy  
354 is available to affect other variables. This might have an effect for impact models, because, as an  
355 example, evapotranspiration might be unrealistically high if precipitation occurs at the same time with  
356 full solar irradiation during noon. In order to reduce possible inconsistencies with other variables that  
357 could lead to implications in impact models, the precipitation is only distributed to hours at nighttime,  
358 Alternatively, we implemented the option for the user to write Not a Number (NaN) values instead.

359 Drizzle precipitation (values below 1 mm day<sup>-1</sup>) is also disaggregated to sub-daily values in order to  
360 ensure mass and energy conservation. If no historical precipitation event is found for this case,  
361 precipitation noise is again randomly distributed to an hour at nighttime. If no hour without radiation  
362 occurs (e.g. high latitudes in northern summer), the precipitation is distributed to local midnight.

363 The calculation procedure can be performed either for universal time (UT) or for local solar time (LST).  
364 The latter divides the world into equal time zones of 15° with the central time zone (+7.5°) at  
365 Greenwich.

#### 366 4. Results

367 In a first step, Teddy is applied for 30 globally distributed samples (Fig. 2) for the year 2010. To be able  
368 to validate the results, we perform a cross-validation. Therefore, WFDE5 data for 2010 aggregated to  
369 daily values serve as an input for Teddy. The same year is excluded from the statistical population  
370 during the cross-validation. As a result, it can be tested how well WFDE5 hourly values for the year  
371 2010 are reproduced with the statistical population of the other 39 years. The 30 samples are chosen  
372 to represent globally relevant agricultural production regions in different climate zones (Fig. 2). To  
373 evaluate the sensitivity of the different DOY window sizes, we run the cross-validation with different  
374 DOY window sizes, ranging from 1 to 25, in steps of two, including the option to disable the DOY  
375 window (DOY window size = 0). In order to additionally validate the performance for extreme events,  
376 we perform a second cross-validation for all available 40 years (1980-2019) with DOY window sizes of  
377 11 for sample location 29, located in Southern Germany.

Gelöscht: physical

Gelöscht: (without solar radiation)

Gelöscht: “

Gelöscht: bias”

Gelöscht: Precipitation

Gelöscht:

Gelöscht: are

Gelöscht: l

Formatiert: Schriftart: Fett

Formatiert: Listenabsatz, Nummerierte Liste + Ebene: 1  
+ Nummerierungsformatvorlage: 1, 2, 3, ... + Beginnen  
bei: 1 + Ausrichtung: Links + Ausgerichtet an: 0,63 cm  
+ Einzug bei: 1,27 cm

[1] nach unten verschoben: Validation¶

Formatiert: Schriftart: Fett

Gelöscht: In a first step, a cross-validation is carried out for  
30 globally distributed samples (Fig. 2) for the year 2010.

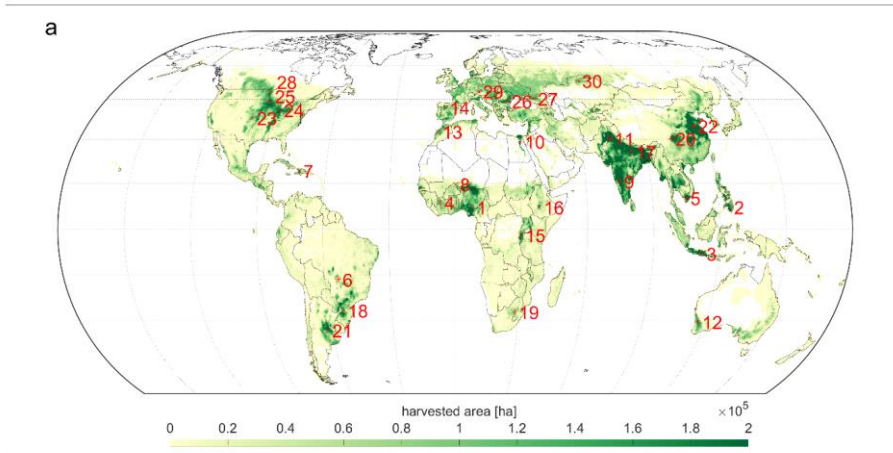
Gelöscht: s

Gelöscht: basic population

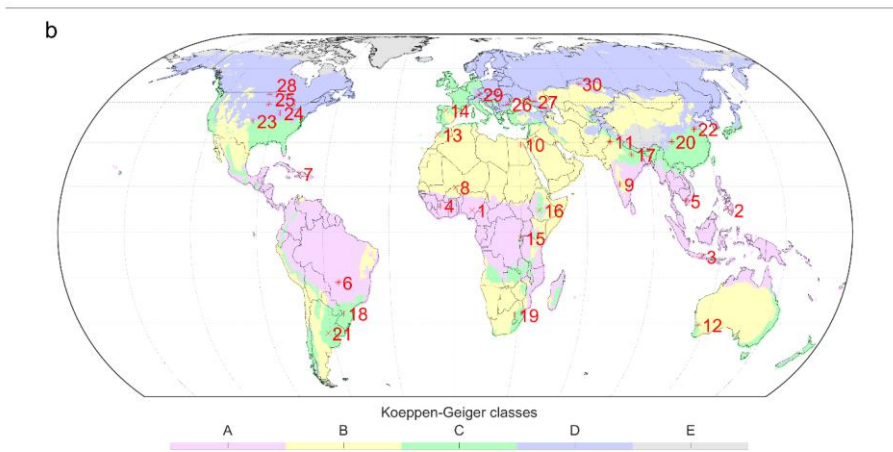
Gelöscht: basic population

Gelöscht: all

Gelöscht: and 25



394



395

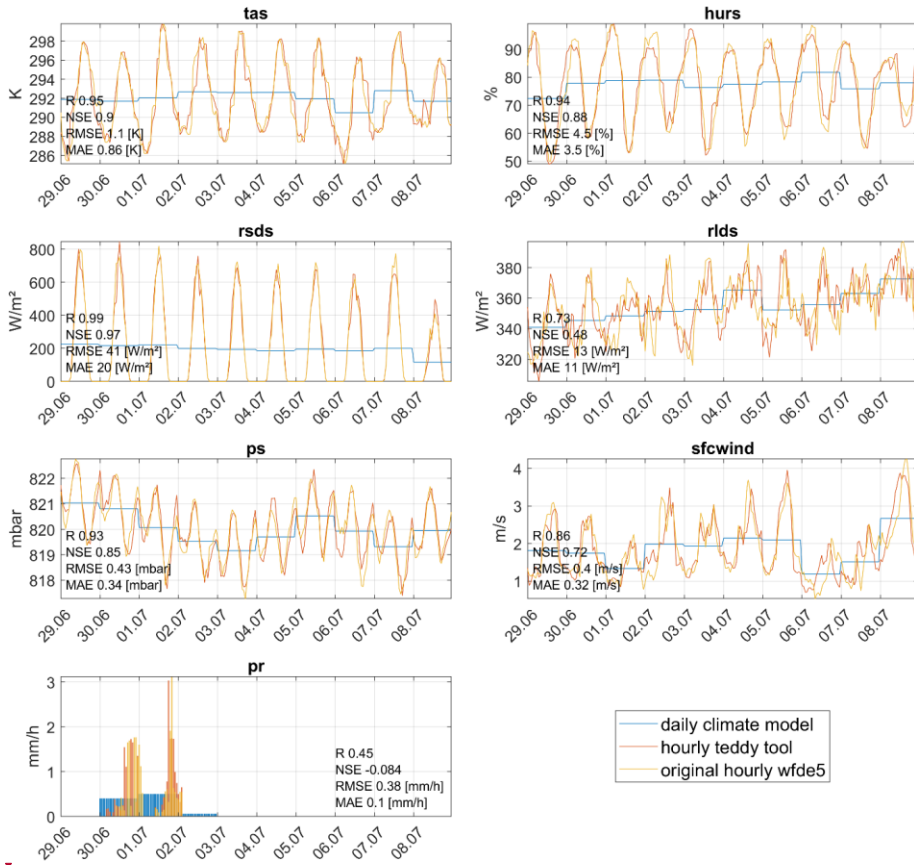
396 Figure 2: Distribution of 30 global samples used for the cross-validation on (a) annual total harvested  
 397 area of rainfed and irrigated crops in hectare per pixel at a 30 arc-minute grid (Portmann et al., 2010)  
 398 and (b) for Koeppen-Geiger climate zones calculated for 1980-2019 WFDE5 temperature and  
 399 precipitation values (Beck et al., 2018). Samples are ordered by climate zone affiliation and their  
 400 distance to the equator.

401 4.1 Validation

402 As an example, for sample location 16 in Ethiopia, Fig. 3 shows the results of the temporal  
 403 disaggregation series for the cross-validation for a 10-day time series in 2010 in comparison with the  
 404 daily climate input and the original hourly WFDE5 data. The hourly courses show high correlations for  
 405 the randomly selected time series for all variables except for precipitation (Fig. 3 and scatterplots in  
 406 Fig. 4 for the entire year; Supplementary Fig. S2 and S3 alternatively show sample location 22 in China).

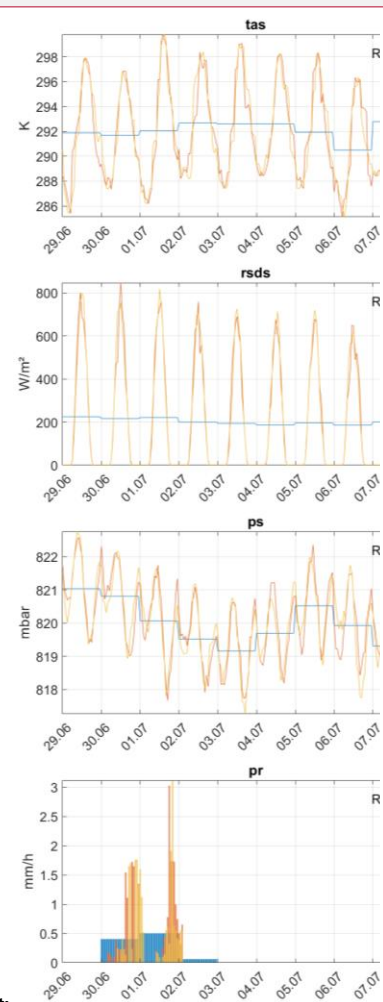
[1] verschoben (Einfügung)  
 Formatiert: Schriftart: Nicht Fett, Unterstrichen  
 Gelöscht: example





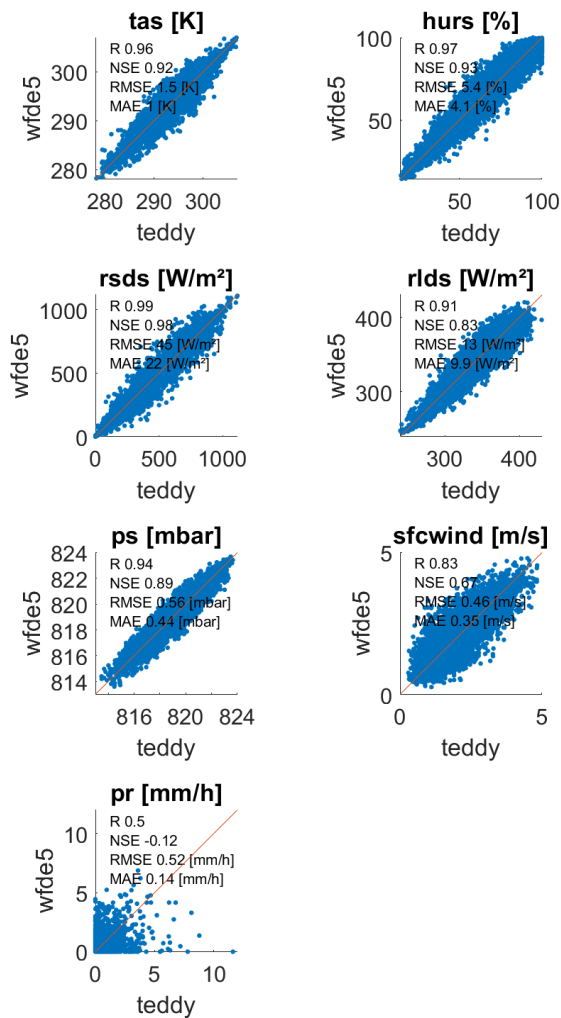
408

409 Figure 3: Time-series for all variables comparing daily climate model data, disaggregated hourly results  
 410 of Teddy from the performed cross-validation and the original hourly WFDE5 data, shown for sample  
 411 location 16 in Ethiopia with a DOY window size of 7 for the 10-day period 29.06. – 08.07.2010. The  
 412 Pearson correlation coefficient (R), the Nash-Sutcliffe model efficiency coefficient (NSE), the root mean  
 413 squared error (RMSE) and the mean absolute error (MAE) are displayed for the shown time period for  
 414 each variable.



Gelöscht:

Gelöscht: is



Gelöscht: ¶

417  
 418 Figure 4: Hourly values for the year 2010 between disaggregated values generated by the Teddy-Tool  
 419 and the original WFDE5 data used for the cross-validation, exemplarily for sample [location](#) 16 in  
 420 Ethiopia with a DOY window size of 7. [The Pearson correlation coefficient \(R\), the Nash-Sutcliffe model](#)  
 421 [efficiency coefficient \(NSE\), the root mean squared error \(RMSE\) and the mean absolute error \(MAE\)](#)  
 422 [are displayed for each variable.](#)

423 4.2 Sensitivity analysis DOY window size

424 The sensitivity analysis averaged over all 30 samples shows that the Pearson correlation coefficient of  
 425 hourly values for the year 2010 show high correlations for all variables ( $r > 0.9$ ), except wind\_speed  
 426 ( $r > 0.7$ ) and precipitation ( $r > 0.4$ ), which are generally [more difficult to disaggregate](#) (Fig. 5;  
 427 [Supplementary Fig. S4 additionally shows the Nash-Sutcliffe model efficiency coefficient](#)). The selected  
 428 DOY window size has an effect on the quality of the results. While no DOY window (size=0) results in

**Formatiert:** Standard, Keine Aufzählungen oder Nummerierungen

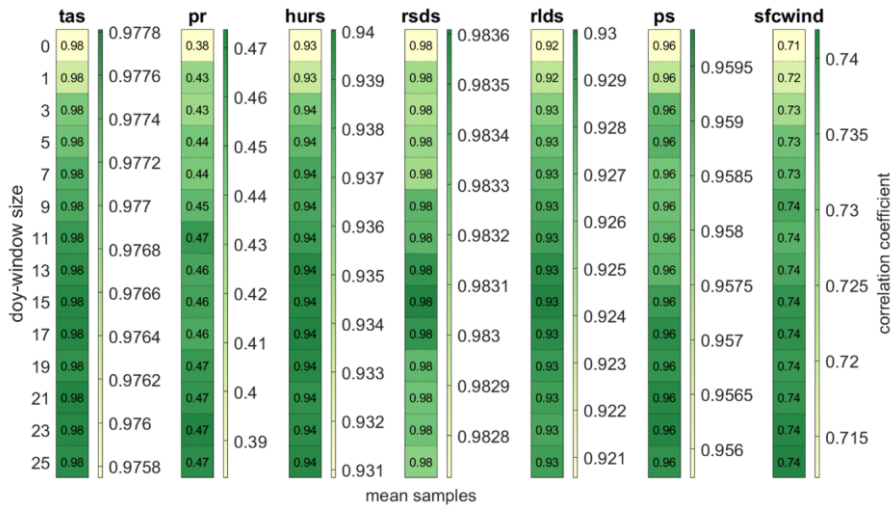
**Formatiert:** Unterstrichen

**Gelöscht:** are the most difficult variables for disaggregation

**Gelöscht:** ).

432 the lowest correlation coefficient across all variables, the DOY window size does significantly affect the  
 433 correlation for precipitation and wind speed (Fig. 5).

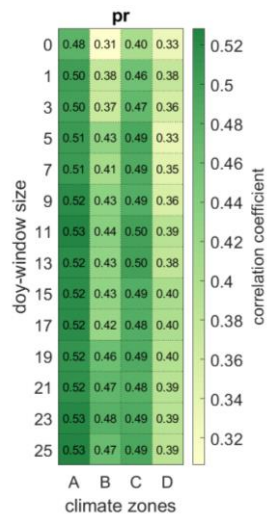
Gelöscht: not  
 Gelöscht: except



434  
 435 Figure 5: Pearson correlation coefficient for different DOY window sizes averaged over all 30 samples  
 436 for the year 2010 for all variables being disaggregated to hourly values. The scaling of the colorbar  
 437 differs between variables.

438 For precipitation, the impact of the DOY window size on the correlation varies between regions. Larger  
 439 DOY windows are mainly beneficial for precipitation in arid regions, while showing lower increases in  
 440 correlation in regions with pronounced seasons (Fig. 6). The results also show that the correlation for  
 441 precipitation is generally larger in tropical regions than in continental regions.

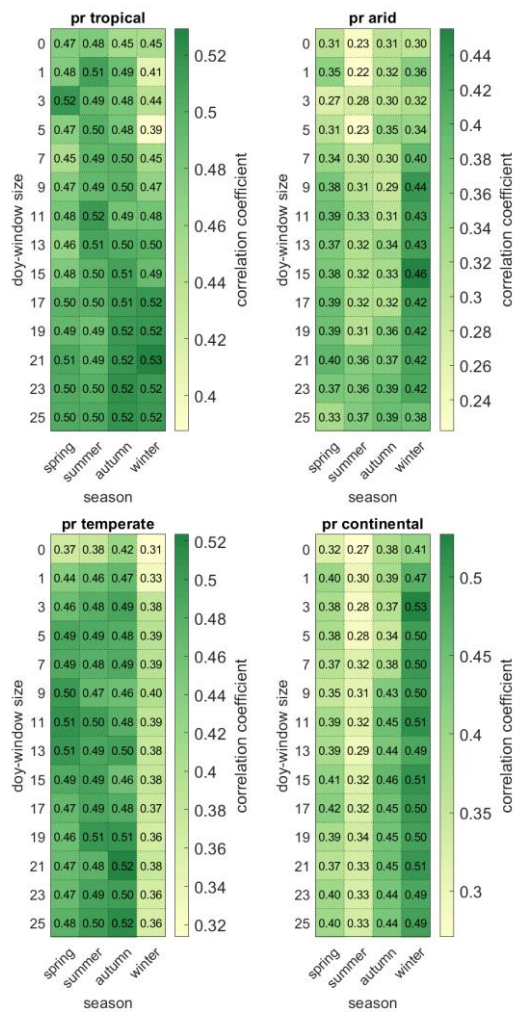
Gelöscht: tropical and  
 Gelöscht:  
 Gelöscht: , the correlation might decrease with larger DOY window size



442

449 Figure 6: Pearson correlation coefficient for different DOY window sizes averaged over the samples for  
 450 each Koeppen-Geiger climate zone (A=tropical, B=arid, C=temperate, D=continental).

451 While hourly precipitation can be best reproduced for winter seasons in continental and arid regions,  
 452 winter seasons show the lowest correlation for temperate regions. Tropical regions only show  
 453 relatively low variations over the year, independently from the selected DOY window size (Fig. 7).  
 454 Especially in arid regions, the length of the DOY window size affects the results differently in different  
 455 seasons. Here, larger DOY windows decrease the correlation during the rainy season (winter and  
 456 spring), while correlation is increased during the dry season (summer and autumn).



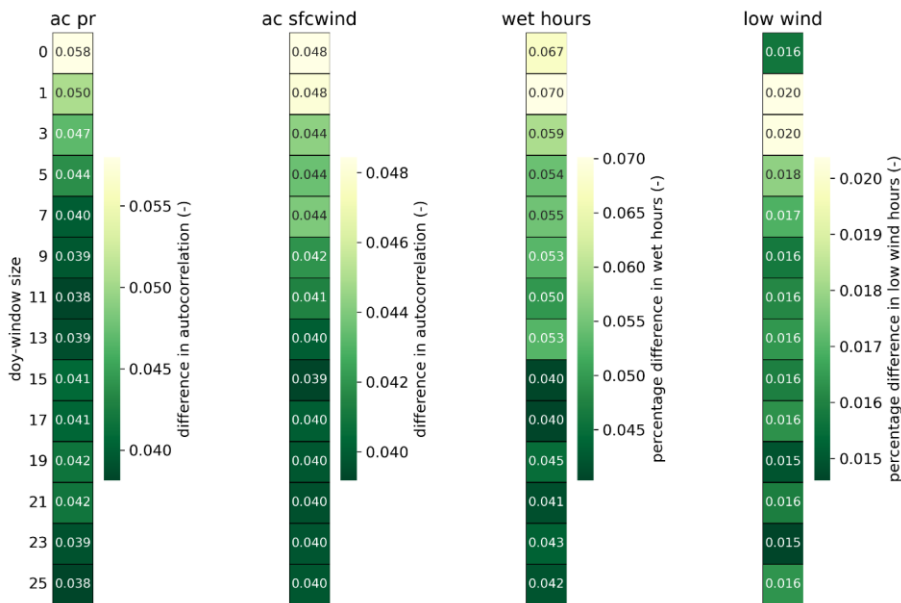
457  
 458 Figure 7: Pearson correlation coefficient for different DOY window sizes averaged over the samples for  
 459 the four seasons (Northern hemisphere: spring=MAM, summer=JJA, autumn=SON, winter=DJF;  
 460 Southern hemisphere: spring=SON, summer=DJF, autumn=MAM, winter=JJA). The heatmap is

**Gelöscht:** The shift of the seasons between Northern and Southern hemisphere is considered.

463 averaged over the samples for each Koeppen-Geiger climate zone (A=tropical, B=arid, C=temperate,  
 464 D=continental).

465 Furthermore, we evaluate the sensitivity of the DOY window size to the reproduction of temporal  
 466 autocorrelation (Fig. 8). Therefore, the autocorrelation over lag times between one and 24 hours is  
 467 calculated for precipitation and wind speed. Autocorrelation refers to the similarity of a time series to  
 468 a lag duration shifted version of the same time series. This allows sub-daily patterns and inter-hour  
 469 connectivity to be statistically captured and validated in time series of precipitation and wind speed.  
 470 In addition, we also check the reproduction of wet hours (precipitation above  $0.1 \text{ mm h}^{-1}$ ) in 2010 and  
 471 the number of hours with low wind speeds (sfcwind <  $2.5 \text{ m s}^{-1}$ ) referring to the typical cut-in wind  
 472 speed of wind turbines.

473 Here, we find that short DOY window sizes below 5 days are not beneficial to all statistics. The  
 474 autocorrelation of precipitation (wind speed) is reproduced more accurately with window sizes of 9  
 475 days or longer. The number of wet hours is better recreated with window sizes above 15 days. For  
 476 hours with low wind speed, a minor improvement is found above 9 days.



477  
 478 Figure 8: Extended validation statistics for the sensitivity analysis of the DOY window size for the year  
 479 2010. The difference in autocorrelation refers to the average over all 30 samples and lag durations  
 480 between one and 24 hours. Wet hours are defined as precipitation intensities above  $0.1 \text{ mm h}^{-1}$  and  
 481 low wind speeds refer to hours with sfcwind <  $2.5 \text{ m s}^{-1}$ .

482 [4.3 Evaluation of the whole period 1980 – 2019](#)

483 [The previous validation has assessed the disaggregation performance for all sample locations for the](#)  
 484 [year 2010 and different DOY window sizes. For the analysis of the whole time period 1980 – 2019, we](#)  
 485 [evaluate the 40-year timeseries for sample location 29 and a window size of 11 days. Figure 9 and](#)

Gelöscht: stations

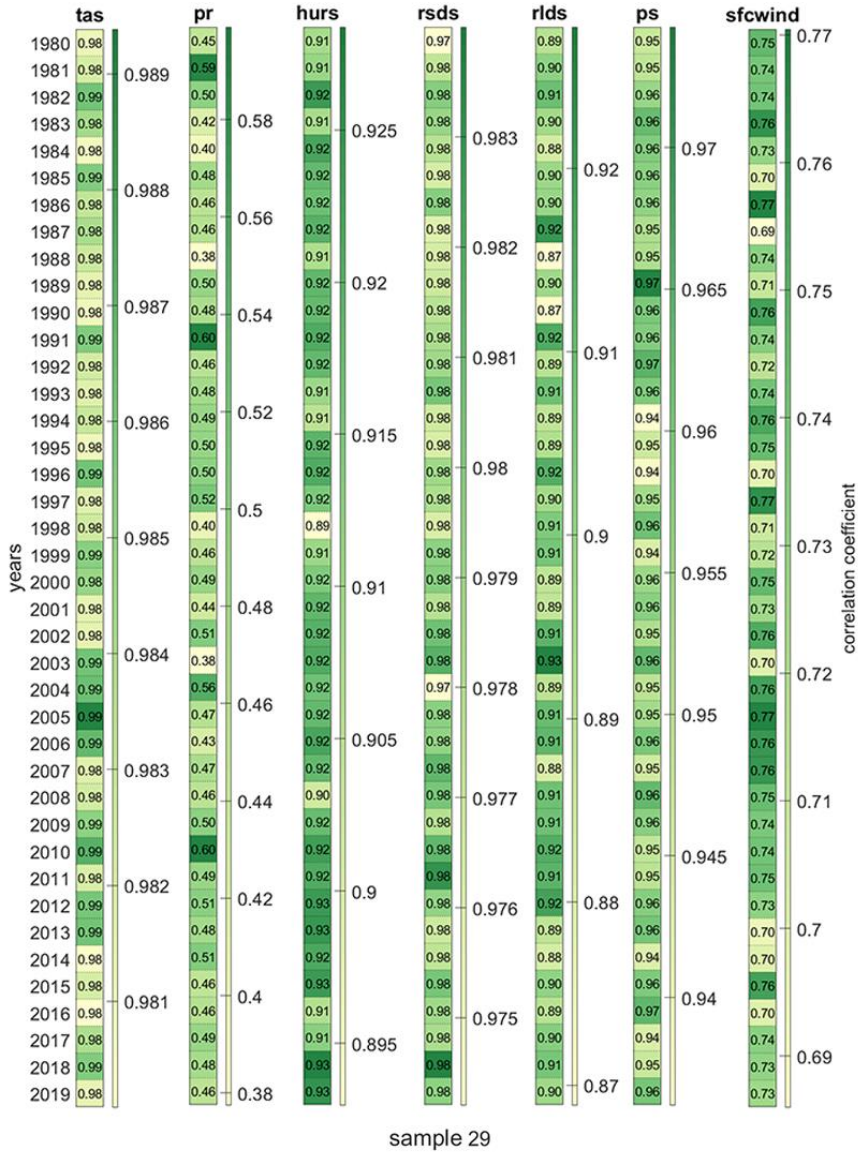
Gelöscht: mm h-1

Gelöscht: m s-1

Gelöscht: ¶  
 ¶  
 ¶  
 ¶

Gelöscht: ¶

495 Supplementary Fig. S5 show the correlation coefficient and mean absolute error, respectively, for each  
 496 year to assess the interannual variability of disaggregation performance. For tas, hurs, rds, rlds, and  
 497 ps the performance shows only very minor differences, whereas sfcwind and pr show a higher degree  
 498 of interannual fluctuations.



499  
 500 **Figure 9:** Pearson correlation coefficient for 1980 – 2019 for sample location 29 and a DOY window  
 501 size of 11 days. The scaling of the colorbar differs between variables.

Gelöscht: s

Gelöscht: the

Gelöscht:

Formatiert: Zentriert

Formatiert: Schriftart: 11 Pt., Nicht Kursiv, Schriftfarbe: Automatisch

Feldfunktion geändert

Gelöscht: 8

Formatiert: Schriftart: 11 Pt., Nicht Kursiv, Schriftfarbe: Automatisch

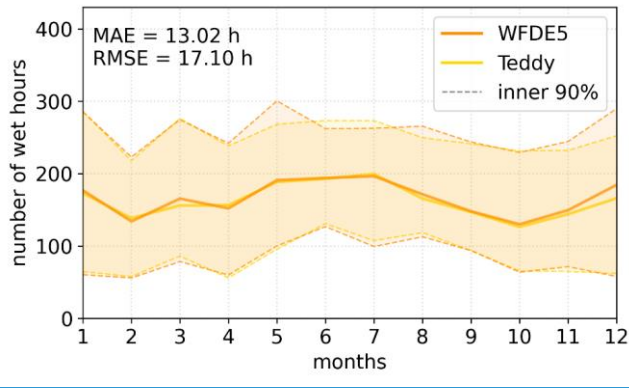
Formatiert: Schriftart: 11 Pt., Nicht Kursiv, Schriftfarbe: Automatisch

Gelöscht: Figure 9:

507 [4.4 Evaluation of precipitation: Wet proportions and intensities](#)

508 [For the further evaluation of precipitation characteristics, also the disaggregated timeseries over the](#)  
509 [whole period 1980 – 2019 for sample location 29 is assessed. In order to evaluate the reproduction of](#)  
510 [wet/dry proportions, the monthly cycle of wet hours is provided \(Fig. 10\). Wet hours above 0.1 mm h<sup>-1</sup>](#)  
511 [are recreated by the Teddy-Tool with minor differences for the median over 40 years \(Fig. 10\). The](#)  
512 [error measures are calculated for every year separately amounting to a mean absolute error of 13.02](#)  
513 [h equaling 7.8 %.](#)

514 [For the evaluation of the range of precipitation intensities, Fig. 11 shows intensities above 1 mm h<sup>-1</sup>](#)  
515 [plotted against its percentage of exceedance for sub-daily durations. We find that the disaggregated](#)  
516 [precipitation intensities match the original data except for extreme precipitation.](#)



517  
518 [Figure 10; Number of wet hours per month for sample location 29 in Germany. Solid lines show the](#)  
519 [median over 40 years, where the dashed lines denote the inner 90% of the 40-year period. MAE and](#)  
520 [RMSE are calculated separately for every year and averaged over 40 years.](#)

521  
522

Gelöscht: ¶  
¶  
¶  
Formatiert: Unterstrichen

Gelöscht: ure

Gelöscht: ¶

Formatiert: Zentriert

Gelöscht: 9

Gelöscht: Figure 10:

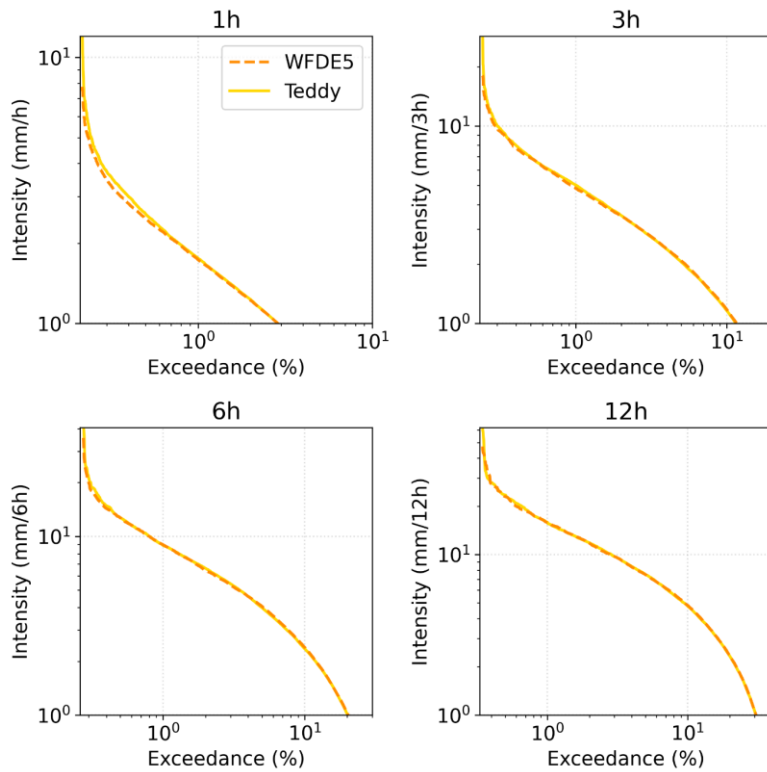


Figure 11: Exceedance probability of precipitation intensities for sub-daily durations for sample location 29 in Germany.

#### 4.5. Evaluation of precipitation extremes

As the ISIMIP data base is used for future impact modelling and historical attribution science (Mengel et al., 2021), extremes are of major interest for the community. The ability of global climate models to simulate sub-daily extremes is limited and depends on the variable of interest and the spatio-temporal conditions of the extreme and the respective model setup (Wehner et al., 2021; Kumar et al., 2015; Wang and Clow, 2020). However, in this validation, we evaluate how the Teddy-Tool is able to preserve the statistics of sub-daily extreme values. Therefore, we select precipitation as variable of interest. Figure 12 shows the reproduction of sub-daily precipitation extremes for 1980 – 2019 for sample location 29 in southern Germany, where Teddy is run with a DOY window size of 11 days. The 40 annual maxima are extracted from the original and the disaggregated data. Additionally, the Generalized Extreme Value (GEV) distribution is fitted to these empirical data. GEV parameters are estimated via Maximum Likelihood Estimation (Coles, 2001), where the goodness-of-fit is assessed with the Anderson-Darling test at 95% significance level (Stephens, 1986). Thereby, 95% confidence intervals are generated applying a bootstrap procedure with 1000 iterations to account for extreme value statistical uncertainties. We find that the Teddy-Tool leads to an overestimation of annual maximum precipitation. For the hourly duration, the differences are large with the confidence intervals of the

Formatiert: Zentriert, Nicht vom nächsten Absatz trennen

Gelöscht: 9

Formatiert: Schriftart: Nicht Kursiv

Formatiert: Schriftart: Nicht Kursiv

Formatiert: Schriftart: Nicht Kursiv

Gelöscht: 11

Formatiert: Schriftart: Nicht Kursiv

Gelöscht: ¶

Formatiert: Unterstrichen

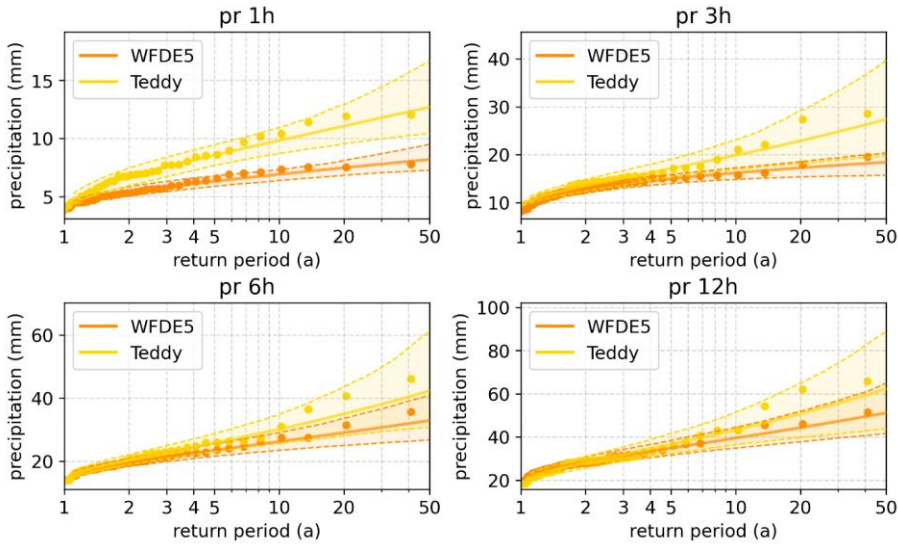
Gelöscht: need to

Gelöscht: 1

Gelöscht:



555 GEV hardly overlapping. For the longer durations, Teddy values approach the original data, with  
 556 noticeable differences only for the rare events with return periods above 5 years.



557  
 558 Figure 12: Extreme value statistical evaluation of sub-daily precipitation for sample location 29 in  
 559 Germany. The annual maxima of the WFDE5 and Teddy are shown as dots. Additionally, GEV fits (lines)  
 560 with 95% confidence intervals (transparent areas and dashed lines) account for uncertainties. The  
 561 Teddy-Tool is run with a DOY window size of 11 days.

### 562 5. Discussion and Outlook

563 The Teddy-Tool allows for temporal disaggregation of daily climate model data. The disaggregation is  
 564 based on location and time specific empirical relationships between variables. The approach is well  
 565 suitable for all tested variables and results in very high correlations (>0.9), except for precipitation  
 566 (>0.5) and wind speed (>0.75). We refer the worse performance for precipitation and wind speed to  
 567 the high intra-day variability for these variables (Watters et al., 2021). Other variables are governed by  
 568 a stronger diurnal cycle (Dai and Trenberth, 2004), which is easier to disaggregate based on empirical  
 569 diurnal profiles.

570 Compared to other approaches, the advantage of the Teddy-Tool is that no other input data is required  
 571 rather than the daily climate model data. The Teddy-Tool is relatively simple to apply, considers specific  
 572 local and seasonal features of the diurnal course of different climate variables, and preserves the  
 573 physical consistency of inter-variable relationships. Mass and energy are conserved and mean daily  
 574 values of the climate model are reproduced any time.

575 The spatial and temporal resolution of the results is determined by the provided temporal and spatial  
 576 resolution of the chosen reference data (WFDE5 used here). Longer available reanalysis time periods  
 577 extend the statistical population for identifying the most similar weather conditions in the past and  
 578 thus could improve the results. Generally, also other reference data could be used, that provides higher  
 579 temporal or spatial resolution for a specific region.

Gelöscht: 9

Gelöscht: Figure 29:

Gelöscht: ¶

Formatiert: Schriftart: Fett

Formatiert: Nummerierte Liste + Ebene: 1 + Nummerierungsformatvorlage: 1, 2, 3, ... + Beginnen bei: 1 + Ausrichtung: Links + Ausgerichtet an: 0,63 cm + Einzug bei: 1,27 cm

Gelöscht: Conclusions

Gelöscht: er

Gelöscht: The o

Gelöscht: regional

Gelöscht: considers

Gelöscht:

Gelöscht: basic population

590 The DOY window to find the most similar historical weather situations can be chosen in different sizes.  
591 For most of the variables, we found small effects of time window adjustments, except for precipitation  
592 and wind speed. The evaluation of different DOY window sizes reveals that a DOY window size of 11  
593 can generally be recommended across all variables. Larger DOY windows should be avoided mainly in  
594 arid regions, while shorter DOY windows generally lead to poorer representations of autocorrelation  
595 and extreme events.

Gelöscht: time

596 One limitation of the Teddy-Tool is the representation of extreme events, mainly for precipitation,  
597 which is generally the most difficult variable for temporal disaggregation. We found that hourly  
598 precipitation extremes are overestimated. For heavy daily precipitation events, Teddy distributes the  
599 24h-sums either correctly, too evenly or on too few hours. When distributing on too few hours,  
600 extreme hourly intensities evolve, which may have never occurred or may even be physically  
601 implausible. For temporal disaggregation of extreme precipitation, we recommend dynamical  
602 downscaling via high-resolution climate models (Poschlod, 2021; Poschlod et al., 2021; Zabel et al.,  
603 2012; Zabel and Mauser, 2013).

Gelöscht:

Gelöscht: not always reproduced

604 Another limitation of the approach is the reproduction of the inter-day connectivity within the  
605 disaggregated time series. When two diurnal profiles are chosen for the disaggregation of adjacent  
606 days, which show dissimilar courses in the time steps at the change of the day, abrupt value jumps  
607 might occur in the disaggregation. This can be seen in Fig. 3 for rlds from July 4<sup>th</sup> to July 5<sup>th</sup>. To illustrate  
608 this issue, a disaggregation time series from another location is provided in Supplementary Fig. S2. This  
609 limitation does also apply for the Method of Fragments applied on precipitation (Li et al., 2018).  
610 Similarly to Li et al. (2018), we also consider the precipitation state of the previous and following day  
611 to improve inter-day connectivity. Without this additional consideration, overnight precipitation  
612 events would often be 'cut off' in the disaggregation. For the remaining abrupt jumps in the  
613 disaggregated time series, we refrain from post-processing with subsequent smoothing, as we want to  
614 preserve both mass and energy and the empirical diurnal profiles.

Gelöscht:

Gelöscht: 4

Formatiert: Hochgestellt

Gelöscht: 5

Formatiert: Hochgestellt

Gelöscht: the

Gelöscht: ure

Gelöscht: 2

Gelöscht: "

Gelöscht: "

Gelöscht:

615 For the disaggregation of future climate projections using of the Teddy-Tool, we have the following  
616 remarks: As the Teddy-Tool derives the relationships between sub-daily and daily values empirically  
617 based on reanalysis data, future diurnal profiles, which are outside the historical range of diurnal  
618 profiles, might possibly be not fully reproduced. However, this limitation is common for statistical  
619 approaches, which are to be calibrated on historical data (Papalexioi et al., 2018). Nevertheless, due  
620 to energy and mass conservation, climate trends in the daily climate signal are fully preserved. Hence,  
621 applying Teddy for temporal disaggregation under climate change holds under the assumption that we  
622 select the most similar meteorological day of the historical data and that this diurnal profile is  
623 representative for future climatic conditions. However, this assumption might apply to a different  
624 degree for different variables. We expect non-stationarity for the diurnal profiles due to changing  
625 weather patterns, shifts in rainfall generating processes, and shifts in the seasonality, mainly for  
626 precipitation and wind. The daily course of other variables, such as solar radiation and temperature  
627 might generally be less affected by a warmer climate. Furthermore, global climate models at coarse  
628 resolutions generally do not represent all processes to fully reproduce intra-day variability. Teddy  
629 applies the diurnal profiles and intra-day variability from the WFDE5 data, which are bias-adjusted  
630 ERA5 reanalysis data that implicitly consider finer scale effects than coarse-resolution global climate  
631 models (Cucchi et al., 2020). Thus, the disaggregation process in Teddy is consistent with the bias  
632 adjustment in ISIMIP3.

645 Another limitation of the methodology could occur in the case of strong climate change signals. In case  
 646 of high warming in end-of-century projections, the number of sampled historical days might decrease  
 647 if the same historical day is sampled repeatedly. This could lead to reductions in diversity of the diurnal  
 648 profile. Hence, Teddy allows to monitor the number of unique analogue days per year. An additional  
 649 analysis for SSP3-7.0 using the GFDL-ESM4 climate model shows that the number of unique analogue  
 650 climate days are declining, as expected, but still the diversity of chosen days is above 300 unique days  
 651 at the end of the century for a chosen moving-window size of  $\pm 11$  days (Supplementary Fig. S6). A  
 652 smaller size of the moving window prevents that the same analogue day is chosen over a longer time  
 653 period. This will increase the diversity of diurnal profiles at the expense of similarity. Even if diurnal  
 654 profiles are derived from the same analogue day repeatedly, the disaggregated diurnal courses, e.g.  
 655 for temperature, will show variations (different offset and different amplitude) due to conservation of  
 656 daily mean energy and mass. From a broader perspective, it is also not clear whether the uncertainties  
 657 resulting from this limitation are larger than the uncertainties within the climate model projections  
 658 until the end of the century. Furthermore, in the long term, the basic population for finding analogue  
 659 climates will continuously increase, since WFDE5 data, which are based on ERA5, are continuously  
 660 updated. We note that Teddy could be also employed to disaggregate future daily climate projections  
 661 based on hourly future climate projections as reference.

662 Further possible developments could include improvements for the reproduction of the inter-day  
 663 connectivity. Despite the consideration of precipitation classes, still abrupt value jumps over day  
 664 changes are possible. A future introduction of temperature classes and surface pressure classes in  
 665 addition to the precipitation classes could help to reduce this effect. Depending on the location of  
 666 interest, also including climate modes or weather patterns for the choice of the most similar  
 667 meteorological day could positively affect the performance. Furthermore, depending on the  
 668 application, it could be reasonable not to screen for the most similar meteorological day, but for the  
 669 most similar succession of multiple days. This would as a consequence improve the inter-day  
 670 connectivity as less different profiles are selected.

671 Other optional future developments could include the separation of direct and diffuse radiation, which  
 672 is also a required information for some impact models which is currently not provided by ISIMIP.  
 673 However, we would make further development with more options dependent on the community's  
 674 adoption of the current executable tool.

#### 675 Code availability

676 The source code of the Teddy-Tool (v1.1) and a parallelized version of the Teddy-Tool (v1.1p), including  
 677 a precompiled executable file for Windows, preprocessed data, results of the cross-validation and  
 678 exemplary results for SSP 585 (2015 – 2100) and the UKESM1-0-L climate model for 30 samples are  
 679 provided via Zenodo (<https://doi.org/10.5281/zenodo.8124111>).

#### 680 Author contribution

681 FZ: Conceptualization, Software, Methodology, Validation, Formal analysis, Resources, Data curation,  
 682 Writing - original draft, Visualization

683 BP: Methodology, Validation, Formal analysis, Writing - original draft, Visualization

#### 684 Competing interests

- Formatiert: Standard
- Gelöscht: In order to prevent for high warming
- Formatiert: Nicht Hervorheben
- Formatiert: Nicht Hervorheben
- Gelöscht: that
- Gelöscht: , which
- Formatiert: Nicht Hervorheben
- Formatiert: Nicht Hervorheben
- Formatiert: Nicht Hervorheben
- Gelöscht:
- Formatiert: Nicht Hervorheben
- Formatiert: Nicht Hervorheben
- Formatiert: Nicht Hervorheben
- Formatiert: Schriftfarbe: Automatisch
- Gelöscht: Since mass and energy are conserved within the disaggregation approach, the
- Gelöscht: might
- Gelöscht: despite the diurnal profile are derived from the same analogue day
- Gelöscht:
- Gelöscht: an improved
- Gelöscht: changes
- Gelöscht: improve

700 The contact author has declared that none of the authors has any competing interests.

#### 701 Acknowledgements

702 We acknowledge the methodological discussion with Stefan Lange from the Potsdam Institute of  
703 Climate Impact Research (PIK).

#### 704 References

- 705 Alliot, P., Allard, D., Monbet, V., and Naveau, P.: Stochastic weather generators: an overview of  
706 weather type models, *Journal de la société française de statistique*, 156, <https://doi.org/101-113>,  
707 2015.
- 708 Beck, H. E., Zimmermann, N. E., McVicar, T. R., Vergopolan, N., Berg, A., and Wood, E. F.: Present and  
709 future Köppen-Geiger climate classification maps at 1-km resolution, *Scientific Data*, 5, 180214,  
710 <https://doi.org/10.1038/sdata.2018.214>, 2018.
- 711 [Bennett, A., Hamman, J. & Nijssen, B.: MetSim: A python package for estimation and disaggregation  
712 of meteorological data, \*Journal of Open Source Software\*, 5\(47\), 2042,  
713 <https://doi.org/10.21105/joss.02042>, 2020.](https://doi.org/10.21105/joss.02042)
- 714 Breinl, K. and Di Baldassarre, G.: Space-time disaggregation of precipitation and temperature across  
715 different climates and spatial scales, *Journal of Hydrology: Regional Studies*, 21, 126-146,  
716 <https://doi.org/10.1016/j.ejrh.2018.12.002>, 2019.
- 717 Buck, A. L.: New Equations for Computing Vapor Pressure and Enhancement Factor, *Journal of*  
718 *Applied Meteorology and Climatology*, 20, 1527-1532, [https://doi.org/10.1175/1520-0450\(1981\)020<1527:Nefcvp>2.0.Co;2](https://doi.org/10.1175/1520-0450(1981)020<1527:Nefcvp>2.0.Co;2), 1981.
- 720 Byers, E., Gidden, M., Leclère, D., Balkovic, J., Burek, P., Ebi, K., Greve, P., Grey, D., Havlik, P., Hillers,  
721 A., Johnson, N., Kahil, T., Krey, V., Langan, S., Nakicenovic, N., Novak, R., Obersteiner, M.,  
722 Pachauri, S., Palazzo, A., Parkinson, S., Rao, N. D., Rogelj, J., Satoh, Y., Wada, Y., Willaarts, B., and  
723 Riahi, K.: Global exposure and vulnerability to multi-sector development and climate change  
724 hotspots, *Environmental Research Letters*, 13, 055012, <https://doi.org/10.1088/1748-9326/aabf45>, 2018.
- 725  
726 Chen, D., Dai, A., and Hall, A.: The Convective-To-Total Precipitation Ratio and the “Drizzling” Bias in  
727 Climate Models, *Journal of Geophysical Research: Atmospheres*, 126, e2020JD034198,  
728 <https://doi.org/10.1029/2020JD034198>, 2021.
- 729 [Chen, C. J.: Temporal disaggregation of seasonal forecasting for streamflow simulation. \*World  
730 Environmental and Water Resources Congress 2016\*, pp. 63-72, 2016.](https://doi.org/10.1007/978-1-4471-3675-0_2001)
- 731 [Coles, S.: \*An Introduction to Statistical Modeling of Extreme Values\*. Springer, London, U.K.  
732 \[https://doi.org/10.1007/978-1-4471-3675-0\\\_2001\]\(https://doi.org/10.1007/978-1-4471-3675-0\_2001\).](https://doi.org/10.1007/978-1-4471-3675-0_2001)
- 733 Colón-González, F. J., Sewe, M. O., Tompkins, A. M., Sjödin, H., Casallas, A., Rocklöv, J., Caminade, C.,  
734 and Lowe, R.: Projecting the risk of mosquito-borne diseases in a warmer and more populated  
735 world: a multi-model, multi-scenario intercomparison modelling study, *The Lancet Planetary  
736 Health*, 5, e404-e414, [https://doi.org/10.1016/S2542-5196\(21\)00132-7](https://doi.org/10.1016/S2542-5196(21)00132-7), 2021.
- 737 Cucchi, M., Weedon, G. P., Amici, A., Bellouin, N., Lange, S., Müller Schmied, H., Hersbach, H., and  
738 Buontempo, C.: WFDE5: bias-adjusted ERA5 reanalysis data for impact studies, *Earth Syst. Sci.  
739 Data*, 12, 2097-2120, <https://doi.org/10.5194/essd-12-2097-2020>, 2020.
- 740 [Dai, A. and Trenberth, K. E.: The Diurnal Cycle and Its Depiction in the Community Climate System  
741 Model. \*Journal of Climate\*, 17, 930-951, \[https://doi.org/10.1175/1520-0442\\(2004\\)017<0930:TDCAID>2.0.CO;2\]\(https://doi.org/10.1175/1520-0442\(2004\)017<0930:TDCAID>2.0.CO;2\), 2004.](https://doi.org/10.1175/1520-0442(2004)017<0930:TDCAID>2.0.CO;2)
- 742  
743 Debele, B., Srinivasan, R., and Yves Parlange, J.: Accuracy evaluation of weather data generation and  
744 disaggregation methods at finer timescales, *Advances in Water Resources*, 30, 1286-1300,  
745 <https://doi.org/10.1016/j.advwatres.2006.11.009>, 2007.
- 746 Degife, A. W., Zabel, F., and Mauser, W.: Climate change impacts on potential maize yields in  
747 Gambella region, Ethiopia, *Regional Environmental Change*, <https://doi.org/10.1007/s10113-021-01773-3>, 2021.
- 748

Formatiert: Absatz-Standardschriftart

Formatiert: Absatz-Standardschriftart

749 Eyring, V., Bony, S., Meehl, G. A., Senior, C. A., Stevens, B., Stouffer, R. J., and Taylor, K. E.: Overview  
750 of the Coupled Model Intercomparison Project Phase 6 (CMIP6) experimental design and  
751 organization, *Geosci. Model Dev.*, 9, 1937-1958, <https://doi.org/10.5194/gmd-9-1937-2016>, 2016.

752 Förster, K., Hanzer, F., Winter, B., Marke, T., and Strasser, U.: An open-source MEteoroLOGical  
753 observation time series DIAggregation Tool (MELODIST v0.1.1), *Geosci. Model Dev.*, 9, 2315-  
754 2333, <https://doi.org/10.5194/gmd-9-2315-2016>, 2016.

755 Franke, J. A., Müller, C., Minoli, S., Elliott, J., Folberth, C., Gardner, C., Hank, T., Izaurrealde, R. C.,  
756 Jägermeyr, J., Jones, C. D., Liu, W., Olin, S., Pugh, T. A. M., Ruane, A. C., Stephens, H., Zabel, F., and  
757 Moyer, E. J.: Agricultural breadbaskets shift poleward given adaptive farmer behavior under  
758 climate change, *Global Change Biol.*, 28, 167-181, <https://doi.org/10.1111/gcb.15868>, 2022.

759 Golub, M., Thiery, W., Marcé, R., Pierson, D., Vanderkelen, I., Mercado-Bettin, D., Woolway, R. I.,  
760 Grant, L., Jennings, E., Kraemer, B. M., Schewe, J., Zhao, F., Frieler, K., Mengel, M., Bogomolov, V.  
761 Y., Bouffard, D., Côté, M., Couture, R. M., Debolskiy, A. V., Droppers, B., Gal, G., Guo, M., Janssen,  
762 A. B. G., Kirillin, G., Ladwig, R., Magee, M., Moore, T., Perroud, M., Piccolroaz, S., Raaman Vinnaa,  
763 L., Schmid, M., Shatwell, T., Stepanenko, V. M., Tan, Z., Woodward, B., Yao, H., Adrian, R., Allan,  
764 M., Anneville, O., Arvola, L., Atkins, K., Boegman, L., Carey, C., Christianson, K., de Eyto, E.,  
765 DeGasperi, C., Grechushnikova, M., Hejzlar, J., Joehnk, K., Jones, I. D., Laas, A., Mackay, E. B.,  
766 Mammarella, I., Markensten, H., McBride, C., Özkundakci, D., Potes, M., Rinke, K., Robertson, D.,  
767 Rusak, J. A., Salgado, R., van der Linden, L., Verburg, P., Wain, D., Ward, N. K., Wollrab, S., and  
768 Zdorovenova, G.: A framework for ensemble modelling of climate change impacts on lakes  
769 worldwide: the ISIMIP Lake Sector, *Geosci. Model Dev.*, 15, <https://doi.org/4597-4623>,  
770 <https://doi.org/10.5194/gmd-15-4597-2022>, 2022.

771 Görner, C., Franke, J., Kronenberg, R., Hellmuth, O., and Bernhofer, C.: Multivariate non-parametric  
772 Euclidean distance model for hourly disaggregation of daily climate data, *Theoretical and Applied  
773 Climatology*, 143, 241-265, <https://doi.org/10.1007/s00704-020-03426-7>, 2021.

774 Jägermeyr, J., Müller, C., Ruane, A. C., Elliott, J., Balkovic, J., Castillo, O., Faye, B., Foster, I., Folberth,  
775 C., Franke, J. A., Fuchs, K., Guarin, J. R., Heinke, J., Hoogenboom, G., Iizumi, T., Jain, A. K., Kelly, D.,  
776 Khabarov, N., Lange, S., Lin, T.-S., Liu, W., Mialyk, O., Minoli, S., Moyer, E. J., Okada, M., Phillips,  
777 M., Porter, C., Rabin, S. S., Scheer, C., Schneider, J. M., Schyns, J. F., Skalsky, R., Smerald, A., Stella,  
778 T., Stephens, H., Webber, H., Zabel, F., and Rosenzweig, C.: Climate impacts on global agriculture  
779 emerge earlier in new generation of climate and crop models, *Nature Food*, 2, 873-885,  
780 <https://doi.org/10.1038/s43016-021-00400-y>, 2021.

781 [Juckes, M., Taylor, K. E., Durack, P. J., Lawrence, B., Mizielinski, M. S., Pamment, A., Peterschmitt, J.-](https://doi.org/10.5194/gmd-13-201-2020)  
782 [Y., Rixen, M., and Sénési, S.: The CMIP6 Data Request \(DREQ, version 01.00.31\), \*Geosci. Model\*  
783 \[Dev.\]\(https://doi.org/10.5194/gmd-13-201-2020\), 13, 201-224, <https://doi.org/10.5194/gmd-13-201-2020>, 2020.](https://doi.org/10.5194/gmd-13-201-2020)

784 Kumar, D., Mishra, V., and Ganguly, A. R.: Evaluating wind extremes in CMIP5 climate models,  
785 *Climate Dynamics*, 45, 441-453, <https://doi.org/10.1007/s00382-014-2306-2>, 2015.

786 Kunstmann, H. and Stadler, C.: High resolution distributed atmospheric-hydrological modelling for  
787 Alpine catchments, *Journal of Hydrology*, 314, 105-124,  
788 <https://doi.org/10.1016/j.jhydrol.2005.03.033>, 2005.

789 Lange, S.: Trend-preserving bias adjustment and statistical downscaling with ISIMIP3BASD (v1.0),  
790 *Geosci. Model Dev.*, 12, 3055-3070, <https://doi.org/10.5194/gmd-12-3055-2019>, 2019.

791 Li, X., Meshgi, A., Wang, X., Zhang, J., Tay, S. H. X., Pijcke, G., Manocha, N., Ong, M., Nguyen, M. T.,  
792 and Babovic, V.: Three resampling approaches based on method of fragments for daily-to-subdaily  
793 precipitation disaggregation, *International Journal of Climatology*, 38, e1119-e1138,  
794 <https://doi.org/10.1002/joc.5438>, 2018.

795 Liston, G. E. and Elder, K.: A Meteorological Distribution System for High-Resolution Terrestrial  
796 Modeling (MicroMet), *Journal of Hydrometeorology*, 7, 217-234,  
797 <https://doi.org/10.1175/jhm486.1>, 2006.

798 Liu, C., Ikeda, K., Thompson, G., Rasmussen, R., and Dudhia, J.: High-Resolution Simulations of  
799 Wintertime Precipitation in the Colorado Headwaters Region: Sensitivity to Physics

800 Parameterizations, *Monthly Weather Review*, 139, 3533-3553, <https://doi.org/10.1175/MWR-D-11-00009.1>, 2011.

801 [Lüttgau, J., Kunkel, J.: Cost and Performance Modeling for Earth System Data Management and Beyond. In: Yokota, R., Weiland, M., Shalf, J., Alam, S. \(eds\) High Performance Computing. ISC High Performance 2018. Lecture Notes in Computer Science, vol 11203. Springer, Cham.](#)

802 [https://doi.org/10.1007/978-3-030-02465-9\\_2](https://doi.org/10.1007/978-3-030-02465-9_2), 2018.

803

804 Mengel, M., Treu, S., Lange, S., and Frieler, K.: ATTRICI v1.1 – counterfactual climate for impact attribution, *Geosci. Model Dev.*, 14, 5269-5284, <https://doi.org/10.5194/gmd-14-5269-2021>,

805 2021.

806 [Meredith, E., Ulbrich, U., Rust, H. W., and Truhetz, H.: Present and future diurnal hourly precipitation in 0.11° EURO-CORDEX models and at convection-permitting resolution, \*Environmental Research Communications\*, 3, 055002, <https://doi.org/10.1088/2515-7620/abf15e>, 2021.](#)

807

808

809 Mezghani, A. and Hingray, B.: A combined downscaling-disaggregation weather generator for stochastic generation of multisite hourly weather variables over complex terrain: Development and multi-scale validation for the Upper Rhone River basin, *Journal of Hydrology*, 377, 245-260, <https://doi.org/10.1016/j.jhydrol.2009.08.033>, 2009.

810

811 Minoli, S., Jägermeyr, J., Asseng, S., Urfels, A., and Müller, C.: Global crop yields can be lifted by timely adaptation of growing periods to climate change, *Nature Communications*, 13, 7079, <https://doi.org/10.1038/s41467-022-34411-5>, 2022.

812

813 Orlov, A., Daloz, A. S., Sillmann, J., Thiery, W., Douzal, C., Lejeune, Q., and Schleussner, C.: Global Economic Responses to Heat Stress Impacts on Worker Productivity in Crop Production, *Economics of Disasters and Climate Change*, 5, 367-390, <https://doi.org/10.1007/s41885-021-00091-6>, 2021.

814

815 Orlov, A., et al.: Human heat stress could offset economic benefits of the CO2 fertilisation effect in crop production. *Nature Communications: Under Review*, 2023.

816

817 Papalexioiu, S. M., Markonis, Y., Lombardo, F., AghaKouchak, A., and Foufoula-Georgiou, E.: Precise Temporal Disaggregation Preserving Marginals and Correlations (DiPMaC) for Stationary and Nonstationary Processes, *Water Resources Research*, 54, 7435-7458, <https://doi.org/10.1029/2018WR022726>, 2018.

818

819 Park, H. and Chung, G.: A Nonparametric Stochastic Approach for Disaggregation of Daily to Hourly Rainfall Using 3-Day Rainfall Patterns, *Water*, 12, 2306, 2020.

820

821 Portmann, F. T., Siebert, S., and Döll, P.: MIRCA2000—Global monthly irrigated and rainfed crop areas around the year 2000: A new high-resolution data set for agricultural and hydrological modeling, *Global Biogeochemical Cycles*, 24, <https://doi.org/10.1029/2008GB003435>, 2010.

822

823 Poschlod, B.: Using high-resolution regional climate models to estimate return levels of daily extreme precipitation over Bavaria, *Nat. Hazards Earth Syst. Sci.*, 21, 3573-3598, <https://doi.org/10.5194/nhess-21-3573-2021>, 2021.

824

825 [Poschlod, B.: Attributing heavy rainfall event in Berchtesgadener Land to recent climate change – Further rainfall intensification projected for the future, \*Weather Clim Extremes\*, 38, 100492, <https://doi.org/10.1016/j.wace.2022.100492>, 2022.](#)

826

827

828 Poschlod, B. and Ludwig, R.: Internal variability and temperature scaling of future sub-daily rainfall return levels over Europe, *Environmental Research Letters*, 16, 064097, <https://doi.org/10.1088/1748-9326/ac0849>, 2021.

829

830 Poschlod, B., Ludwig, R., and Sillmann, J.: Ten-year return levels of sub-daily extreme precipitation over Europe, *Earth Syst. Sci. Data*, 13, 983-1003, <https://doi.org/10.5194/essd-13-983-2021>, 2021.

831

832 Poschlod, B., Hodnebrog, Ø., Wood, R. R., Alterskjær, K., Ludwig, R., Myhre, G., and Sillmann, J.: Comparison and Evaluation of Statistical Rainfall Disaggregation and High-Resolution Dynamical Downscaling over Complex Terrain, *Journal of Hydrometeorology*, 19, 1973-1982, <https://doi.org/10.1175/jhm-d-18-0132.1>, 2018.

833

834 [Pui, A., Sharma, A., Mehrotra, R., Sivakumar, B., and Jeremiah, E.: A comparison of alternatives for daily to sub-daily rainfall disaggregation, \*J. Hydrol.\*, 470, 138– 157, <https://doi.org/10.1016/j.jhydrol.2012.08.041>, 2012.](#)

835

836

837

838

839

840

841

842

843

844

845

846

847

848

849

850

851

Kommentiert [ZF1]: Currently still under review.

Formatiert: Absatz-Standardschriftart

Formatiert: pagelast

852 Reed, C., Anderson, W., Kruczkiwicz, A., Nakamura, J., Gallo, D., Seager, R., and McDermid, S. S.: The  
853 impact of flooding on food security across Africa, *Proceedings of the National Academy of*  
854 *Sciences*, 119, e2119399119, <https://doi.org/10.1073/pnas.2119399119>, 2022.

855 [Sharma, A. and Srikanthan, S.: Continuous Rainfall Simulation: A Nonparametric Alternative, in:](#)  
856 [30th Hydrology & Water Resources Symposium: Past, Present & Future, 4–7 December 2006,](#)  
857 [Launceston, Tasmania, p. 86, 2006.](#)

858 [Stephens, A. M.: Tests based on EDF statistics. In: D'Agostino, R. B. and Stephens, M. A. \(eds.\):](#)  
859 [Goodness-of-fit techniques, 1986.](#)

860 Sun, Y., Solomon, S., Dai, A., and Portmann, R. W.: How Often Does It Rain?, *Journal of Climate*, 19,  
861 <https://doi.org/916-934>, 10.1175/jcli3672.1, 2006.

862 Tittensor, D. P., Novaglio, C., Harrison, C. S., Heneghan, R. F., Barrier, N., Bianchi, D., Bopp, L.,  
863 Bryndum-Buchholz, A., Britten, G. L., Büchner, M., Cheung, W. W. L., Christensen, V., Coll, M.,  
864 Dunne, J. P., Eddy, T. D., Everett, J. D., Fernandes-Salvador, J. A., Fulton, E. A., Galbraith, E. D.,  
865 Gascuel, D., Guiet, J., John, J. G., Link, J. S., Lotze, H. K., Maury, O., Ortega-Cisneros, K., Palacios-  
866 Abrantes, J., Petrik, C. M., du Pontavice, H., Rault, J., Richardson, A. J., Shannon, L., Shin, Y.-J.,  
867 Steenbeek, J., Stock, C. A., and Blanchard, J. L.: Next-generation ensemble projections reveal  
868 higher climate risks for marine ecosystems, *Nat Clim Change*, 11, 973-981,  
869 <https://doi.org/10.1038/s41558-021-01173-9>, 2021.

870 Trinanes, J. and Martinez-Urtaza, J.: Future scenarios of risk of *Vibrio* infections in a warming planet:  
871 a global mapping study, *The Lancet Planetary Health*, 5, e426-e435,  
872 [https://doi.org/10.1016/S2542-5196\(21\)00169-8](https://doi.org/10.1016/S2542-5196(21)00169-8), 2021.

873 Verfaillie, D., Déqué, M., Morin, S., and Lafaysse, M.: The method ADAMONT v1.0 for statistical  
874 adjustment of climate projections applicable to energy balance land surface models, *Geosci.*  
875 *Model Dev.*, 10, 4257-4283, <https://doi.org/10.5194/gmd-10-4257-2017>, 2017.

876 Vormoor, K. and Skaugen, T.: Temporal Disaggregation of Daily Temperature and Precipitation Grid  
877 Data for Norway, *Journal of Hydrometeorology*, 14, 989-999, [https://doi.org/10.1175/jhm-d-12-](https://doi.org/10.1175/jhm-d-12-0139.1)  
878 [0139.1](https://doi.org/10.1175/jhm-d-12-0139.1), 2013.

879 Wang, K. and Clow, G. D.: The Diurnal Temperature Range in CMIP6 Models: Climatology, Variability,  
880 and Evolution, *Journal of Climate*, 33, 8261-8279, <https://doi.org/10.1175/jcli-d-19-0897.1>, 2020.

881 Warszawski, L., Frieler, K., Huber, V., Piontek, F., Serdeczny, O., and Schewe, J.: The Inter-Sectoral  
882 Impact Model Intercomparison Project (ISI-MIP): Project framework, *Proceedings of the National*  
883 *Academy of Sciences*, 111, 3228-3232, <https://doi.org/10.1073/pnas.1312330110>, 2014.

884 [Watters, D., Battaglia, A., and Allan, R.: The Diurnal Cycle of Precipitation according to Multiple](#)  
885 [Decades of Global Satellite Observations, Three CMIP6 Models, and the ECMWF Reanalysis,](#)  
886 [Journal of Climate](#), 34, 5063-5080, <https://doi.org/10.1175/JCLI-D-20-0966.1>, 2021.

887 Wehner, M., Lee, J., Risser, M., Ullrich, P., Gleckler, P., and Collins, W. D.: Evaluation of extreme sub-  
888 daily precipitation in high-resolution global climate model simulations, *Philosophical Transactions*  
889 *of the Royal Society A: Mathematical, Physical and Engineering Sciences*, 379, 20190545,  
890 <https://doi.org/10.1098/rsta.2019.0545>, 2021.

891 Zabel, F. and Mauser, W.: 2-way coupling the hydrological land surface model PROMET with the  
892 regional climate model MM5, *Hydrology and Earth System Sciences*, 17, 1705–1714,  
893 <https://doi.org/10.5194/hess-17-1705-2013>, 2013.

894 Zabel, F., Mauser, W., Marke, T., Pfeiffer, A., Zängl, G., and Wastl, C.: Inter-comparison of two land-  
895 surface models applied at different scales and their feedbacks while coupled with a regional  
896 climate model, *Hydrology and Earth System Sciences*, 16, 1017–1031,  
897 <https://doi.org/10.5194/hess-16-1017-2012>, 2012.

898 Zabel, F., Müller, C., Elliott, J., Minoli, S., Jägermeyr, J., Schneider, J. M., Franke, J. A., Moyer, E., Dury,  
899 M., Francois, L., Folberth, C., Liu, W., Pugh, T. A. M., Olin, S., Rabin, S. S., Mauser, W., Hank, T.,  
900 Ruane, A. C., and Asseng, S.: Large potential for crop production adaptation depends on available  
901 future varieties, *Global Change Biol*, 27, 3870-3882 <https://doi.org/10.1111/gcb.15649>, 2021.

902 Zhao, W., Kinouchi, T., and Nguyen, H. Q.: A framework for projecting future intensity-duration-  
903 frequency (IDF) curves based on CORDEX Southeast Asia multi-model simulations: An application

Formatiert: Absatz-Standardschriftart

904 for two cities in Southern Vietnam, *Journal of Hydrology*, 598, 126461,  
905 <https://doi.org/10.1016/j.jhydrol.2021.126461>, 2021.